ACS APPLIED ELECTRONIC MATERIALS

Article

Cite This: ACS Appl. Electron. Mater. 2020, 2, 103−110

pubs.acs.org/acsaelm

3,7-Bis(2-oxoindolin-3-ylidene)benzo[1,2-*b*:4,5-*b*′]difuran-2,6-dione Dicyanides with Engineered Side Chains for Unipolar n-Type Transistors

Jianping Lu,*[,†] Afshin Dadvand,[†] Ta-Ya Chu,[†] Mark R. Bortolus,[†] Raluca Movileanu,[†] Jean-Marc Baribeau,[†] Ye Tao,*[,†] Jesse Quinn,[‡] and Yuning Li[‡]

[†]Advanced Electronic and Photonic Research Centre, National Research Council of Canada, Ottawa, Ontario K1A 0R6, Canada

[‡]Department of Chemical Engineering, University of Waterloo, 200 University Ave West, Waterloo, Ontario N2L 3G1, Canada

Supporting Information

ABSTRACT: Air-stable solution-processable unipolar n-type organic semiconductors are highly desired in the field of organic thin film transistors as n-type transistors are indispensable components in low-power-consumption complementary integrated circuits. The present work seeks to address this issue and describes the synthesis of two dicyano-substituted bis(2-oxoindolin-3-ylidene)benzodifurandione (BOIBDD) derivatives with engineered alkyl side chains for n-type transistors. Two kinds of side chains are used in this study: 2-hexyldecyl ($C_{16}H_{33}$) and 3-hexylundecyl ($C_{17}H_{35}$). Surprisingly, the small structural difference between side chains induced remarkable differences in the physical properties and electronic performance of the BOIBDD derivatives. In addition, cyano substitution into the backbone of BOIBDD derivatives was shown to be effective at lowering the HOMO and LUMO energy levels of BOIBDD derivatives to obtain unipolar n-type materials. Compared with fluorine substitution, cyano substitution was readily realized by a simple and straightforward reaction using cheap CuCN as a cyanation reagent. Both atomic force microscopy (AFM) and X-ray diffraction (XRD) studies have confirmed that the BOIBDD derivative with 3-hexylundecyl side chains tended to form highly crystalline structures in the solid state. More interestingly, thermal annealing of this compound at a temperature as low as 75 °C, well below its melting point of 305 °C, can still further improve its crystallinity and thus significantly increase its electron mobility by 43 times to 0.1 $cm^2\ V^{-1}\ s^{-1}$ in air. The insight gained from this study will shed some light on the design of new air-stable high-performance n-type organic semiconductors.

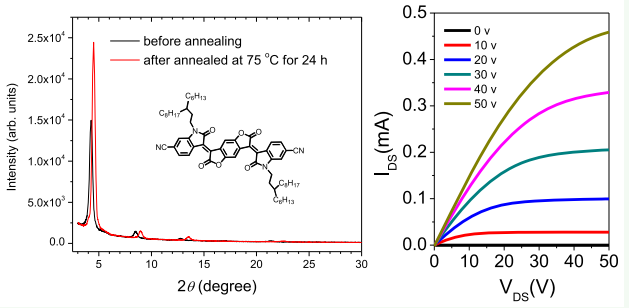

KEYWORDS: *unipolar n-type transistors, bis(2-oxoindolin-3-ylidene)benzodifurandione derivatives, cyano substitution, side-chain engineering, thermal annealing, electron mobility in air*

INTRODUCTION

Organic electronic devices have been intensely investigated in both academia and industry over the past two decades because of their promising potential for broad commercial applications, nonlimiting examples of which include organic light-emitting diodes,[1,2] field effect transistors,[3,4] solar cells,[5,6] and chemo-/biosensors.[7,8] Moreover, organic electronics can be fabricated on plastic substrates to enable lightweight, flexible, and even wearable electronic devices. Such devices typically comprise organic semiconducting materials which are used as thin active layers. Tuning of the physical and optoelectronic properties of conjugated polymers through chemical modification of their backbones has resulted in a wide variety of promising materials for organic electronics applications. Indeed, with polymer solar cells (PSC) with power conversion efficiencies (PCE) exceeding 15%,[9] organic field effect transistors (OFETs) with hole mobilities up to 20 $cm^2\ V^{-1}\ s^{-1}$,[10] and electron mobilities as high as 7.0 $cm^2\ V^{-1}\ s^{-1}$,[11] conjugated polymers now show performances suitable for commercial applications.

Significant advance has been made in p-type materials with hole mobility surpassing that of amorphous silicon.[3,4,10] However, major challenges remain in developing solution-processable, air-stable electron-transporting (n-type) organic materials with low processing temperatures (≤150 °C), which is crucial to allow the use of flexible and inexpensive poly(ethylene terephthalate) (PET) substrates. To achieve air-stable electron transport in organic semiconductors, their LUMO energy levels are required to be below −4.1 eV.[12] For example, one of the best commercially available n-type materials P(NDI2OD-T2) (available from Polyera) exhibits good electron mobility above 0.1 $cm^2\ V^{-1}\ s^{-1}$ in bottom-

Received: September 13, 2019
Accepted: December 4, 2019
Published: December 4, 2019

DOI: 10.1021/acsaelm.9b00594
ACS Appl. Electron. Mater. 2020, 2, 103−110

contact top-gated transistors,[13,14] but its electron mobility decreased to 0.01 $cm^2 V^{-1} s^{-1}$ in bottom-contact bottom-gated transistors. Moreover, because of its high-lying LUMO energy level (−3.9 eV), the unprotected device lost its performance in just a few hours following its exposure to air.[15] Therefore, the development of air-stable unipolar n-type semiconductors with good solubility in organic solvents at room temperature remains of paramount importance in the field of organic electronics.

In recent years, bis(2-oxoindolin-3-ylidene)-benzodifurandione (BOIBDD) has attracted a lot of interest as an important building block for the preparation of high-performance organic semiconductors due to its unique coplanar structure, with its backbone conformation locked by intramolecular hydrogen bonding.[16,17] Moreover, the work from Pei's group demonstrated that fluorine substitution effectively lowered both the HOMO and LUMO energy levels of BOIBDD derivatives, resulting in materials exhibiting air-stable electron transport.[18,19] The BOIBDD derivative comprising four fluorine atoms was shown to exhibit the best performance. Notwithstanding the promising results obtained with fluorine substitutions, the synthesis of multi-fluorinated compounds remains complicated and quite costly.

Cyano functionalization has been reported in the literature to tune the energy levels of organic conjugated materials.[20,21] In this work, we demonstrate that cyano substitution into the backbone of BOIBDD with CuCN as a cyanation reagent is a low-cost and effective method to lower the HOMO and LUMO energy levels of BOIBDD derivatives to produce unipolar n-type organic semiconductors. Unlike fluorine substitution, cyano substitution increases the effective conjugation length and thus decreases the optical bandgap of BOIBDD derivatives from 2.3 to 1.8 eV. We work on side-chain engineering in this work as well. It is well-known that side chains play a critical role in optimizing the performance of organic electronic devices because of their significant impacts on the solubility and on the molecular packing of crystalline materials. The incorporation of specific side chains has even been reported to influence the material stability of organic semiconductors.[22] Two kinds of side chains are used in this study. One is 2-hexyldecyl ($C_{16}H_{33}$), and the other one is 3-hexylundecyl ($C_{17}H_{35}$). The difference between these two side chains is very small except one additional carbon atom is inserted between the side-chain branching point and the conjugated backbone in 3-hexylundecyl, as shown in Scheme 1. It is interesting to point out that such a small structural difference leads to a significant difference in the crystallization behavior and eventually in the transistor performance. Both BOIBDD-2CN-C_{16} and BOIBDD-2CN-C_{17} exhibited unipolar electron transport with remarkably low threshold voltages (2−5 V) due to their low-lying LUMO energy level (− 4.4 eV below vacuum energy level). However, the average electron mobility of BOIBDD-2CN-C_{16} only reached 0.015 $cm^2 V^{-1} s^{-1}$. On the contrary, the electron mobility of BOIBDD-2CN-C_{17} was more than 6 times higher, reaching 0.1 $cm^2 V^{-1} s^{-1}$. Our finding suggests that bis(2-oxoindolin-3-ylidene)-benzodifurandione dicyanide derivatives are promising n-type materials. In addition, side chains play a critical role in optimizing the performance of small molecule based organic semiconductors because they have direct impacts on the intermolecular packing motifs, film-forming properties, and device performance.

Scheme 1. Chemical Structures of the n-Type Materials Synthesized in This Study

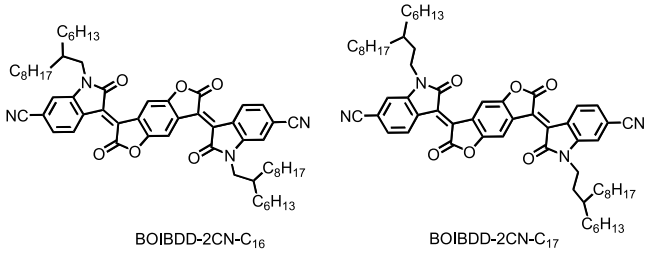

EXPERIMENTAL SECTION

Materials. All starting materials, unless otherwise specified, were purchased from Sigma-Aldrich Co. and used without further purification. Column chromatography was performed on silica gel (size 40−63 μm, pore size 60 Å, Silicycle). Benzo[1,2-*b*:4,5-*b*′]difuran-2,6(3*H*,7*H*)-dione[16] and 7-(2-iodoethyl)pentadecane were synthesized according to the literature methods.[23] The synthetic route to bis(2-oxoindolin-3-ylidene)benzodifurandione dicyanides BOIBDD-2CN-C_{16} and BOIBDD-2CN-C_{17} is shown in Scheme 2, and their detailed synthetic procedures are described below.

Scheme 2. Synthetic Route to Bis(2-oxoindolin-3-ylidene)benzodifurandione Dicyanides with Engineered Side Chains

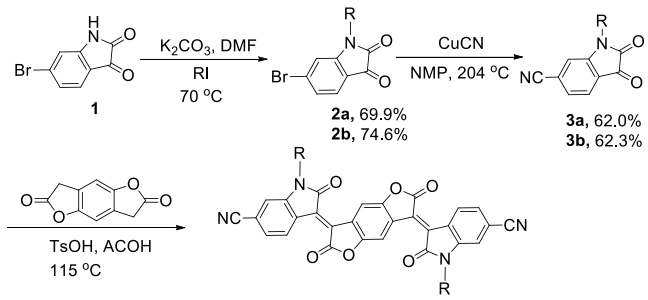

General Procedure for the Alkylation of Isatin (2a, 2b). To a 100 mL three-neck flask equipped with a condenser were added 6-bromoisatin (0.678 g, 3 mmol) and K_2CO_3 (0.828 g, 6 mmol). The system was flushed with argon three times. Then, alkyl iodide (RI, 3.375 mmol) and anhydrous DMF (20 mL) were added via a syringe. The reaction mixture was stirred at 70 °C under argon for 15 h. After cooling, the solvent was removed by distillation under vacuum. The resulting residue was dissolved in chloroform (50 mL) and filtered to remove insoluble materials. After removal of the chloroform, a brown oil was obtained. The crude product was purified by silica gel chromatography with dichloromethane as an eluent. The purified product solidified in a refrigerator overnight.

2a: R = 2-hexyldecyl, 0.945 g, 69.9% yield. ^{1}H NMR (C_6D_6, 400 MHz), δ (ppm): 6.78 (d, J = 8.0 Hz, 1H), 6.65 (d, J = 1.2 Hz, 1H), 6.58 (dd, J_1 = 8.0 Hz, J_2 = 1.2 Hz, 1H), 3.11 (d, J = 7.6 Hz, 2H), 1.62 (m, 1H), 1.40−1.10 (m, 24H), 0.94−0.87 (m, 6H).

2b: R = 3-hexylundecyl, 1.04 g, 74.6% yield. ^{1}H NMR (C_6D_6, 400 MHz), δ (ppm): 6.79 (d, J = 8.0 Hz, 1H), 6.60 (dd, J_1 = 8.0 Hz, J_2 = 1.6 Hz, 1H), 6.56 (d, J = 1.6 Hz, 1H), 3.18 (t, J = 7.6 Hz, 2H), 1.40−1.10 (m, 27H), 0.96−0.89 (m, 6H).

General Procedure for the Synthesis of 1-Alkyl-6-cyanoisatin (3a, 3b). In a 50 mL oven-dried one-necked flask, 1-alkylisatin (2 mmol), CuCN (0.36 g, 4 mmol), and 10 mL of NMP were added. The flask was purged three times with argon, and then the reaction mixture was heated to 204 °C in a salt bath under argon. The resulting solution was stirred at this temperature for 4 h. After cooling

DOI: 10.1021/acsaelm.9b00594
ACS Appl. Electron. Mater. 2020, 2, 103−110

to 150 °C, the hot solution was poured into $FeCl_3$ solution (2.0 g dissolved in 15 mL of 2 M HCl solution). After the solution was stirred for 10 min, chloroform (50 mL) was added. The organic layer was separated, washed with 2 M HCl solution (2 × 15 mL) and water (15 mL) successively, and dried over $MgSO_4$. Then, the organic solvents were removed under vacuum. The residue was purified by silica gel chromatography with dichloromethane as an eluent. The purified product solidified in a refrigerator overnight.

3a: R = 2-hexyldecyl, 0.492 g, 62.0% yield. ^{1}H NMR (C_6D_6, 400 MHz), δ (ppm): 6.71 (d, J = 7.6 Hz, 1H), 6.42 (d, J = 1.2 Hz, 1H), 6.34 (dd, J_1 = 7.6 Hz, J_2 = 1.2 Hz, 1H), 3.09 (d, J = 7.6 Hz, 2H), 1.57 (m, 1H), 1.40−1.10 (m, 24H), 0.94−0.87 (m, 6H).

3b: R = 3-hexylundecyl, 0.511 g, 62.3% yield. ^{1}H NMR (C_6D_6, 400 MHz), δ (ppm): 6.70 (d, J = 7.6 Hz, 1H), 6.34 (dd, J_1 = 7.6 Hz, J_2 = 0.8 Hz, 1H), 6.30 (d, J = 0.8 Hz, 1H), 3.15 (t, J = 7.2 Hz, 2H), 1.40−1.15 (m, 27H), 0.96−0.89 (m, 6H).

General Procedure for the Synthesis of Bis(2-oxoindolin-3-ylidene)benzodifurandione Dicyanide Derivatives (4a, 4b). In a 100 mL oven-dried one-necked flask, 1-alkyl-6-cyanoisatins (1.3 mmol), benzodifurandione (0.54 mmol), toluenesulfonic acid (25 mg), and glacial acetic acid (30 mL) were added. The reaction solution was stirred at 115 °C under nitrogen for 18 h. After cooling, the crude product was collected by filtration and then washed with acetic acid and methanol. The product was further purified by silica gel chromatography with 1:4 hexanes/dichloromethane as an eluent. It is worth mentioning that this product tended to stick to the silica gel. As a result, about 30% of the product stayed on the column and was not eluted out.

4a: BOIBDD-2CN-C_{16}: R = 2-hexyldecyl, 0.197 g, 38.6% yield. ^{1}H NMR 400 MHz (C_6D_6), δ (ppm): 9.39 (s, 2H, from the BDD unit), 9.04 (d, J = 8.4 Hz, 2H, in the meta position to CN), 6.76 (dd, J_1 = 8.4 Hz, J_2 = 1.6 Hz, 2H, in the ortho position to CN), 6.62 (d, J = 1.6 Hz, 2H, in the ortho position to CN), 3.33 (d, J = 7.6 Hz, 4H, adjacent to amide), 1.79 (m, 2H), 1.45−1.20 (m, 48H, aliphatic chains), 0.98−0.88 (m, 12H, $4CH_3$). ^{13}C NMR 100 MHz (CD_2Cl_2), δ (ppm): 167.11 (ester), 166.88 (amide), 152.65, 146.72, 135.65, 130.73, 129.38, 127.71, 126.84, 124.64, 118.57, 116.51 (CN), 111.87, 111.64, 45.30, 36.42, 32.22, 32.13, 31.78, 30.32, 30.00, 29.86, 29.64, 26.65, 26.61, 23.01, 22.99, 14.22, 14.20. MS (MALDI-TOF, m/z): M^- 947.4. Anal. Calcd for $C_{60}H_{74}N_4O_6$: C, 76.08; H, 7.87; N, 5.91. Found: C, 75.81; H, 7.72; N, 5.83.

4b: BOIBDD-2CN-C_{17}: R = 3-hexylundecyl, 0.203 g, 38.3% yield. ^{1}H NMR 400 MHz (C_6D_6), δ (ppm): 9.40 (s, 2H, from the BDD unit), 9.03 (d, J = 8.4 Hz, 2H, in the meta position to CN), 6.76 (dd, J_1 = 8.4 Hz, J_2 = 1.6 Hz, 2H, in the ortho position to CN), 6.53 (d, J = 1.6 Hz, 2H, in the ortho position to CN), 3.41 (t, J = 7.6 Hz, 4H, adjacent to amide), 1.45−1.25 (m, 54H), 1.00−0.90 (m, 12H). ^{13}C NMR 100 MHz (CD_2Cl_2), δ (ppm): 166.84, 166.59, 152.53, 146.23, 135.73, 130.84, 129.29, 127.67, 126.85, 124.71, 118.53, 116.55, 111.87, 111.29, 39.08, 35.89, 33.71, 32.27, 31.19, 30.37, 30.03, 30.00, 29.71, 26.92, 26.87, 23.05, 14.24. MS (MALDI-TOF, m/z): M^- 975.4. Anal. Calcd for $C_{62}H_{78}N_4O_6$: C, 76.35; H, 8.06; N, 5.74. Found: C, 76.21; H, 8.13; N, 5.47.

Characterizations. ^{1}H and ^{13}C NMR spectra were recorded on a Varian AS400 spectrometer in deuterated solvents. UV−vis absorption spectra were recorded on a PerkinElmer Lambda 950 UV−vis spectrometer using 1 cm path-length quartz cells. Optical bandgaps were calculated from the onset of the absorption band. Cyclic voltammograms (CV) were recorded on a CHI600E electrochemical analyzer using a pair of platinum disks as the working electrode and counter electrode, respectively, at a scan rate of 50 mV/s. An Ag/Ag^+ electrode (0.01 M of $AgNO_3$ in acetonitrile) was employed as the reference electrode, and 0.1 M tetrabutylammonium hexafluorophosphate (Bu_4NPF_6) in anhydrous and argon-saturated dichloromethane acted as the supporting electrolyte. The BOIBDD derivatives (~20 mg) were dissolved in the anhydrous dichloromethane for the CV measurement. Under these conditions, the onset oxidatoin potential (E^{ox}) of ferrocene was 0.03 V vs Ag/Ag^+. Ferrocene, used as the reference, has a HOMO energy level of −4.8 eV. The LUMO and HOMO energy levels of the materials were determined by using the empirical equations $E_{LUMO} = -(E^{red}_{onset} + 4.77)$ eV and $E_{HOMO} = -(E^{ox}_{onset} + 4.77)$ eV, respectively, where E^{ox}_{onset} and E^{red}_{onset} are the onset potentials for oxidation and reduction relative to the Ag/Ag^+ electrode, respectively. Thermogravimetric analysis (TGA) measurements were performed using a Mettler Toledo TGA SDTA 851e apparatus at a heating rate of 10 °C/min under a nitrogen atmosphere. The temperature of onset degradation (T_d) corresponds to a 1% weight loss. Differential scanning calorimetric (DSC) analyses was performed using a PerkinElmer DSC-7 instrument, calibrated with ultrapure indium at a scanning rate of 10 °C/min under a nitrogen atmosphere.

Thin Film Transistor Fabrication and Characterization. Silicon substrates with SiO_2 gate dielectrics and prepatterned gold electrodes (Fraunhofer chip) were used to fabricate bottom-contact bottom-gated transistors using the procedure in our previous work.[24] Briefly, the substrates were rinsed with acetone and isopropanol and treated by UV ozone. Then the SiO_2 dielectric surface was passivated by using *n*-dodecyltrichlorosilane in anhydrous toluene. After washing with anhydrous toluene and hexanes successively, the substrates were baked at 100 °C for 10 min. Bis(2-oxoindolin-3-ylidene)-benzodifurandione dicyanide derivatives were dissolved in anhydrous chloroform at a concentration of 6 mg/mL and filtered via a 1 μm polytetrafluoroethylene (PTFE) filter inside a glovebox. The spin-coated films were then annealed at 130 and 75 °C for BOIBDD-2CN-C_{16} and BOIBDD-2CN-C_{17}, respectively, in a nitrogen glovebox for 24 h and allowed to slowly cool to room temperature. The output and transfer characteristics of the fabricated transistors were measured in air by using Keithley 4200 semiconductor analyzer. Based on the measured transfer curves, the standard transistor's current−voltage equation was employed to calculate the field effect mobility in the saturation regime.

RESULTS AND DISCUSSION

Material Synthesis. As can be seen from Scheme 2, the synthesis of dicyano-substituted bis(2-oxoindolin-3-ylidene)-benzodifurandione derivatives is quite simple and straightforward in a three-step reaction sequence. In the second step, 6-bromoisatin was readily converted to 6-cyanoistin by using cheap CuCN as a cyanation reagent with a good reaction yield (~62%). Compared with fluorine substitution, this reaction is much simpler. In the last step, 1-alkyl-6-cyanoisatin was reacted with benzodifurandione by a condensation reaction in acetic acid in the presence of a catalyst amount of toluenesulfonic acid. The reaction yield of this step was high (>70%). However, during purification by silica gel chromatography, we found that quite a lot of the product stuck to the silica gel column and could not be eluted out. As a result, the final yield was around 38% after purification. The obtained final compounds BOIBDD-2CN-C_{16} and BOIBDD-2CN-C_{17} were pure, as indicated by their ^{1}H and ^{13}C NMR spectra (see Figures S1 and S2 in the Supporting Information). Herein, we like to point out that the side chains used in this study (2-hexyldecyl and 3-hexylundecyl) almost had no impact on the reactions. Under the same reaction condition, the overall reaction yields of BOIBDD-2CN-C_{16} and BOIBDD-2CN-C_{17} were almost the same. The syntheses of the aforementioned BOIBDD derivatives were also attempted by an alternate route, in which bis(6-bromo-1-(2-hexyldecyl)-2-oxoindolin-3-ylidene)benzodifurandione was synthesized first and subsequently cyanated with CuCN. It was found that the benzodifurandione core was destroyed under the reaction conditions. Therefore, we could not get our desired product via the alternate synthetic route. This also suggests that the benzodifurandione core should be susceptible to the nucleophilic attack.

DOI: 10.1021/acsaelm.9b00594
ACS Appl. Electron. Mater. 2020, 2, 103−110

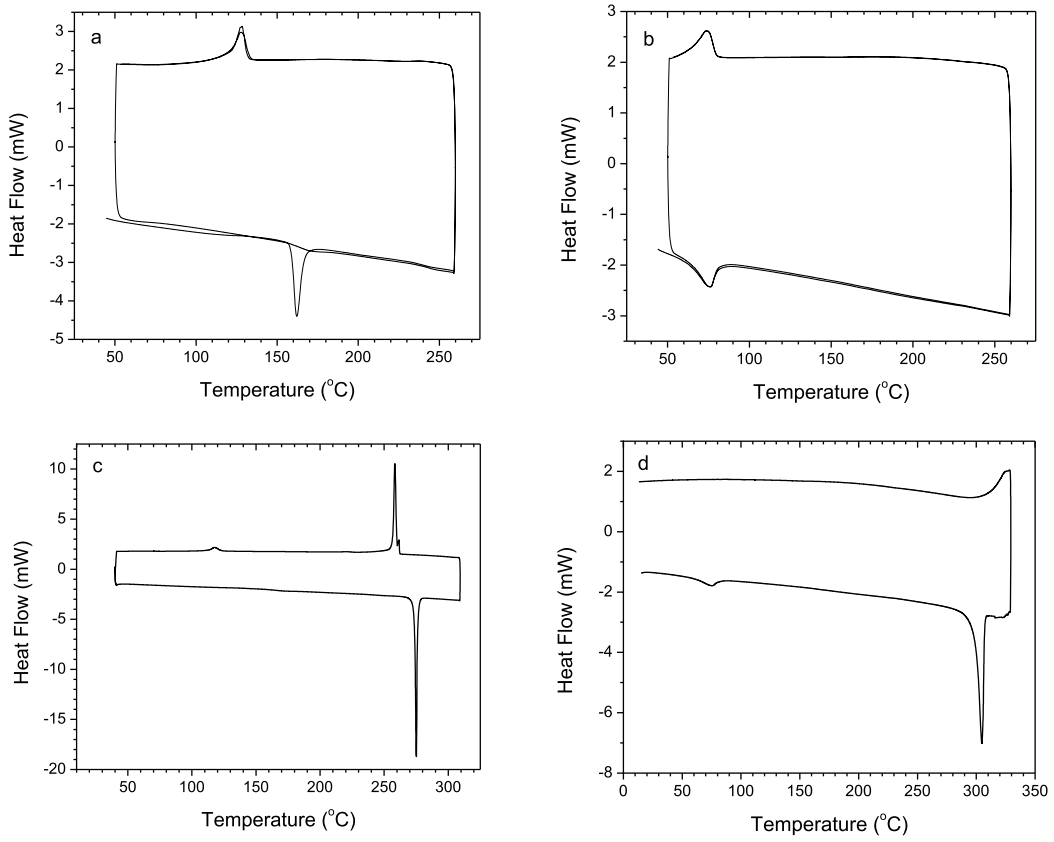

Figure 1. DSC thermograms of BOIBDD-2CN-C_{16} (a, c) and BOIBDD-2CN-C_{17} (b, d). In (c) and (d), the samples were heated to above 300 °C.

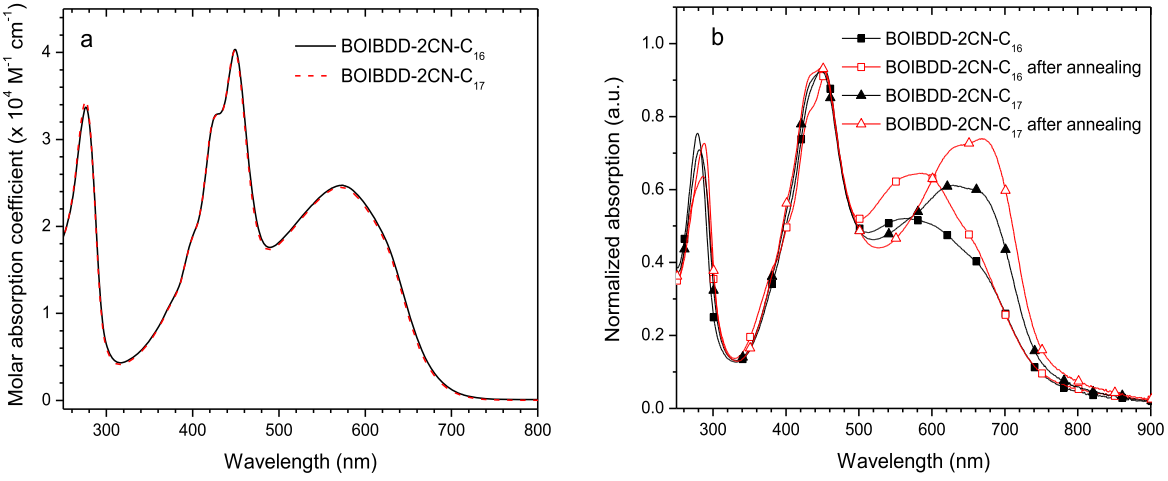

Figure 2. UV−vis absorption spectra of BOIBDD-2CN-C_{16} and BOIBDD-2CN-C_{17} in dichloromethane (a) and in thin films (b).

Physical Properties. The thermal properties of BOIBDD-2CN-C_{16} (C_{16} is 2-hexyldecyl) and BOIBDD-2CN-C_{17} (C_{17} is 3-hexylundecyl) were investigated by DSC. Even though structurally identical, with the exception of the side chains (C_{16} vs C_{17}), the respective DSC thermograms exhibited surprising differences, indicative of the direct impact of the side chains on the thermal behavior of these materials (Figure 1). It has been reported in the literature that side-chain structural modifications can improve the organic semiconductor crystallinity and thus their electron mobility.[25,26] BOIBDD-2CN-C_{16} did not exhibit any melting or crystallizing peaks up to 260 °C in the first DSC scan. A crystallizing and a melting peak, at 128 and 162 °C, respectively, could be observed in the second DSC scan. However, BOIBDD-2CN-C_{17} did exhibit a crystallizing and a melting peak at 74 and 76 °C, respectively, in the first DSC scan. Identical results were obtained in the second DSC scan. Considering that the BOIBDD backbone is quite large and rigid, it is impossible that the backbone of BOIBDD-2CN-C_{17} melted at a temperature as low as 76 °C. This conclusion is further corroborated by the reported melting point of 255 °C for a BOIBDD core comprising a pair of C_8 (2-ethylhexyl) side chains.[19] Because the cyano groups can potentially increase the effective conjugation length of the BOIBDD core structure, it was surmised that BOIBDD-2CN should exhibit a higher melting point. Indeed, heating the samples to higher temperatures in the DSC analysis revealed that BOIBDD-

DOI: 10.1021/acsaelm.9b00594
ACS Appl. Electron. Mater. 2020, 2, 103−110

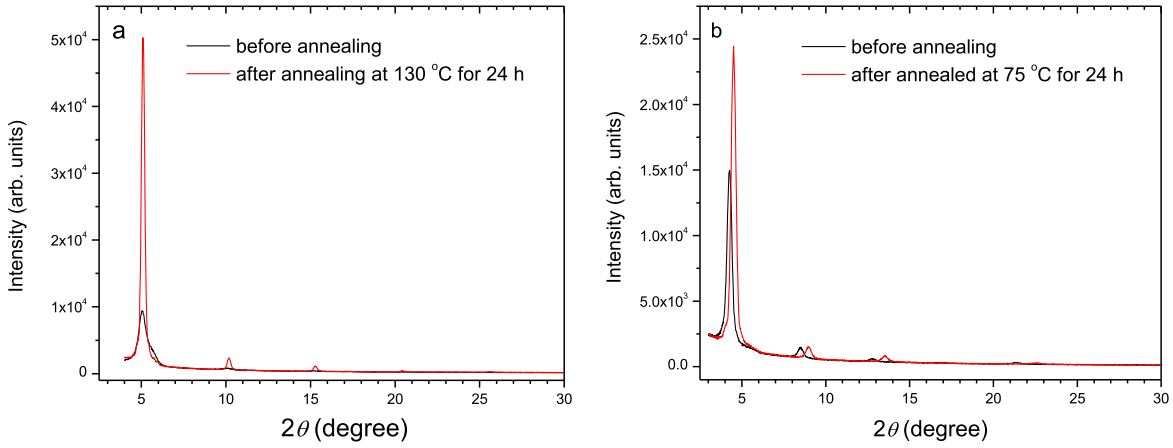

Figure 3. Thin film XRD patterns of BOIBDD-2CN-C_{16} (a) and BOIBDD-2CN-C_{17} (b).

2CN-C_{16} melts at 275 °C while BOIBDD-2CN-C_{17} melts at a temperature as high as 305 °C. Considering these results, it is speculated that the melting points of 76 and 162 °C, as observed for BOIBDD-2CN-C_{17} and BOIBDD-2CN-C_{16}, respectively, correspond to the melting process of the C_{17} and C_{16} side chains. Actually, a similar phenomenon that the side chain and main chain of a polymer melted at different temperatures has been reported in the literature.[27] The difference in observed melting points appears quite large in this study, considering the relatively small structural difference in the respective side chains of BOIBDD-2CN-C_{16} and BOIBDD-2CN-C_{17}. It is very likely that the C_{16} and C_{17} side chains cause these materials to adopt different crystalline structures and packing motifs, which could at least in part account for the better solubility of BOIBDD-2CN-C_{17} in common organic solvents and better film-forming properties. Both materials are relatively stable, and the onset decomposition temperatures (corresponding to 1% weight loss) of BOIBDD-2CN-C_{16} and BOIBDD-2CN-C_{17} were found to be around 329 and 310 °C, respectively. In a summary, the conjugated backbone of BOIBDD-2CN-C_{17} melts at a temperature 30 °C higher than the counterpart BOIBDD-2CN-C_{16}, while the side chains of BOIBDD-2CN-C_{17} melt at a temperature 86 °C lower than the counterpart BOIBDD-2CN-C_{16}. Considering such subtle structural difference in these two compounds, the significant difference in the thermal behaviors is very interesting.

The UV−vis absorption spectra of BOIBDD-2CN-C_{16} and BOIBDD-2CN-C_{17} in dichloromethane were recorded on a PerkinElmer Lambda 950 UV−vis spectrometer. From the onset of their optical absorption, the optical bandgaps of these two compounds were estimated to be 1.81 eV. This bandgap is smaller than those observed for fluorinated BOIBDD (~2.3 eV), implying that the cyano groups indeed increase the effective conjugation length (Figure 2a). It is worth noting that BOIBDD-2CN-C_{16} and BOIBDD-2CN-C_{17} have identical UV−vis absorption spectra, suggesting that the alkyl side chains do not affect the energy bandgaps for this class of materials. Both compounds absorb very strongly in the visible region with molar absorption coefficients of 4.0×10^4 and 2.5×10^4 M^{-1} cm^{-1} at 449 and 573 nm, respectively. However, when these two compounds were processed into thin films by spin-coating, they showed markedly different absorption behaviors. The low-energy absorption peak of BOIBDD-2CN-C_{16} slightly blue-shifted to 560 nm and became broad in the solid state. On the contrary, BOIBDD-2CN-C_{17} exhibited a broad and pronouncedly red-shifted absorption (the absorption peak red-shifted to 628 nm). This suggested that these two compounds adopted different intermolecular packing motifs in the spin-coated films, as manifested in the thermal property study. According to the information obtained from DSC study, BOIBDD-2CN-C_{16} and BOIBDD-2CN-C_{17} films were annealed for 24 h at 130 and 75 °C, respectively. As can be seen from Figure 2b, after annealing the absorption peak of BOIBDD-2CN-C_{16} red-shifts to 587 nm, and the absorption peak of BOIBDD-2CN-C_{17} further red-shifts to 670 nm. Moreover, both BOIBDD-2CN-C_{16} and BOIBDD-2CN-C_{17} showed significantly increased absorption in the long wavelength region, indicating enhanced intermolecular interaction after thermal annealing, consistent with increased crystallization.

X-ray diffraction (XRD) $\theta/2\theta$ scans revealed that the spin-coated BOIBDD-2CN-C_{16} and BOIBDD-2CN-C_{17} films both exhibit a strong first-order diffraction peak, as shown in Figure 3. The peak position corresponds to *d*-spacings of 1.73 and 2.08 nm for BOIBDD-2CN-C_{16} and BOIBDD-2CN-C_{17}, respectively. Besides the first-order diffraction peak, the second and third diffraction peaks are also observed in the BOIBDD-2CN-C_{17} film, indicating a greater degree of molecular ordering even before thermal annealing, relative to BOIBDD-2CN-C_{16}. After thermal annealing, both samples exhibited a stronger first-order diffraction peak together with higher-order diffraction peaks, indicating the molecular ordering was further improved. For BOIBDD-2CN-C_{16}, thermal annealing at 130 °C greatly enhanced the vertical ordering with no significant change in the *d*-spacing. On the contrary, the diffraction peaks of BOIBDD-2CN-C_{17} not only became stronger after annealing at 75 °C but also shifted to higher angles, indicating a reduction of the *d*-spacing (1.96 nm). It seemed that the increased side-chain crystallinity upon thermal annealing enhanced the intermolecular packing and improved the backbone crystallinity. Because no broad diffraction peaks corresponding to intermolecular $\pi-\pi$ stacking were observed for both samples, it is likely that both compounds adopt an edge-on stacking on the substrates. This kind of intermolecular packing is favorable for transistor applications.

AFM study of the spin-coated BOIBDD-2CN-C_{16} film revealed that the film was very smooth before annealing with a surface roughness of ~0.4 nm, and no crystalline structures were observed. After thermal annealing at 130 °C for 24 h, the

DOI: 10.1021/acsaelm.9b00594
ACS Appl. Electron. Mater. 2020, 2, 103−110

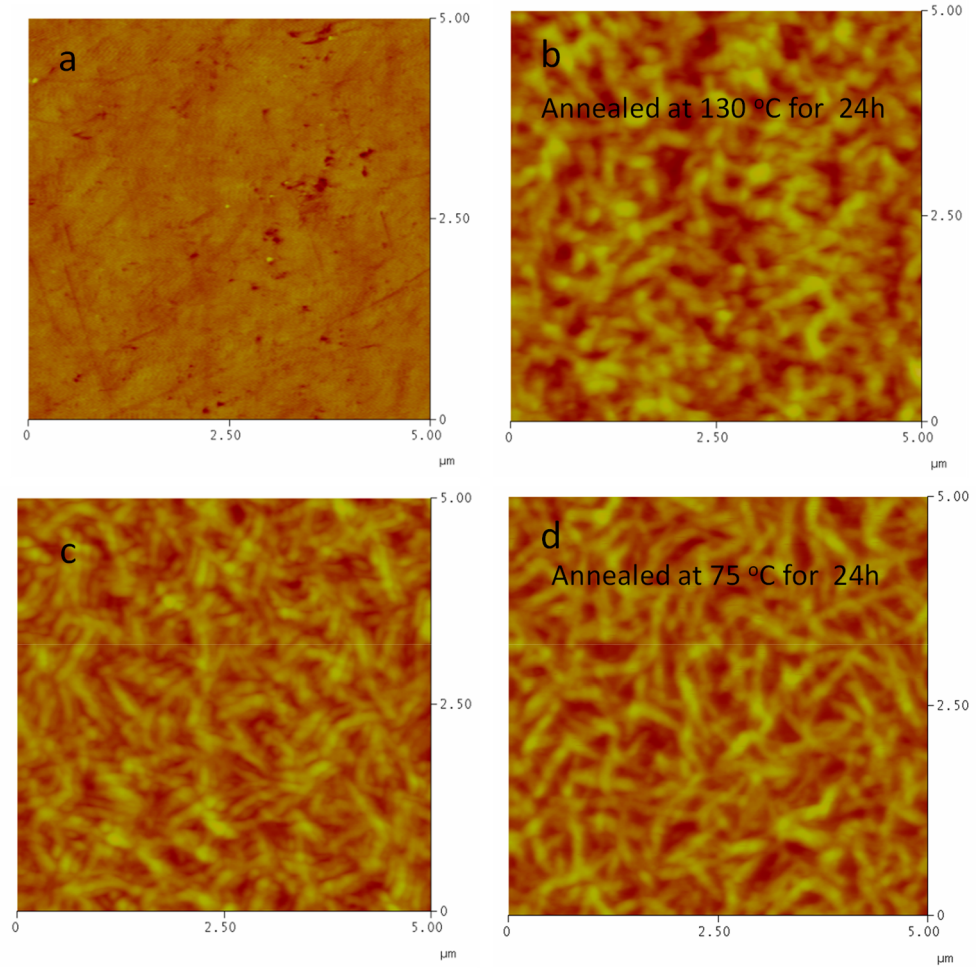

Figure 4. AFM images showing the change in morphology of BOIBDD-2CN-C_{16} (a, b) and BOIBDD-2CN-C_{17} (c, d) upon annealing (a and c before annealing; b and d after annealing).

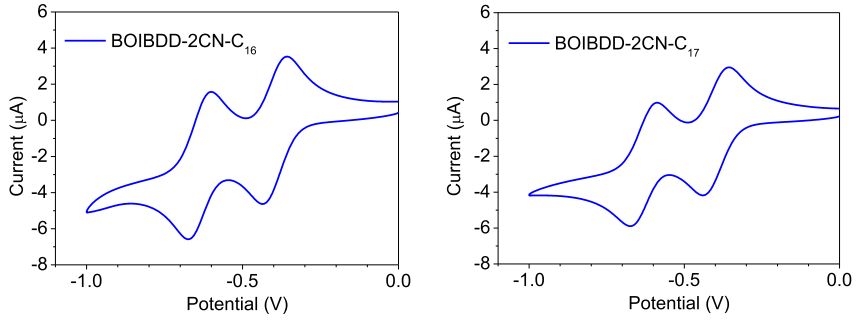

Figure 5. Cyclic voltammograms of BOIBDD-2CN-C_{16} and BOIBDD-2CN-C_{17}. The reference electrode is the Ag/Ag^+ electrode (0.01 M $AgNO_3$ in acetonitrile), which is calibrated with ferrocene.

crystallinity of the film was greatly enhanced, the crystalline grains became larger, and the surface roughness significantly increased to 5.8 nm, as shown in Figure 4. In contrast, AFM images showed that BOIBDD-2CN-C_{17} tended to form crystalline structures with crystalline grains clearly seen in the as spin-coated film. After thermal annealing at 75 °C for 24 h, the crystalline grains became longer, and the surface roughness slightly increased from 8.7 to 9.4 nm.

The HOMO and LUMO energy levels of BOIBDD-2CN-C_{16} and BOIBDD-2CN-C_{17} were investigated by cyclic voltammetry. The materials were dissolved in anhydrous dichloromethane in the CV measurement. Both BOIBDD-2CN-C_{16} and BOIBDD-2CN-C_{17} were readily reduced during the cathodic reduction scan. As shown in Figure 5, the reduction waves are very reversible, and one molecule can accept two electrons. Based on their onset reduction potentials, the LUMO energy levels of BOIBDD-2CN-C_{16} and BOIBDD-2CN-C_{17} were estimated to be −4.45 and −4.44 eV, respectively. These values are 0.80 eV lower than that observed for unsubstituted BOIBDD and are also even lower than the value reported for six fluorinated BOIBDD,[19] suggesting that the cyano group is more effective at lowering the LUMO energy levels of small-molecule organic semiconductors. Oxidation peaks could not be observed during the CV

DOI: 10.1021/acsaelm.9b00594
ACS Appl. Electron. Mater. 2020, 2, 103−110

measurements, indicating that hole injection into this class of materials is difficult and implying that these materials are unipolar n-type materials. The HOMO energy levels were estimated from their LUMO energy levels and optical bandgaps to be ca. −6.26 and −6.25 eV for BOIBDD-2CN-C_{16} and BOIBDD-2CN-C_{17}, respectively.

Bottom-Contact and Bottom-Gated Transistors. Silicon chips with thermal SiO_2 gate dielectrics and patterned gold electrodes from the Fraunhofer Institute are widely used because they can provide reliable, quick, and reproducible estimation of charge mobility in organic semiconductors. In this study, the channel width and length of the transistors are 1 cm and 20 μm, respectively. As both compounds have very good solubility in chloroform (>40 mg/mL), active layer solutions were prepared by dissolving BOIBDD-2CN-C_{16} or BOIBDD-2CN-C_{17} in anhydrous chloroform at a concentration of 6 mg/mL in a nitrogen glovebox. It is well-known that the surface traps of dielectric layers have a detrimental effect on the electron transport; therefore, the SiO_2 surface in this study was passivated with *n*-dodecyltrichlorosilane. To complete device fabrication, the active material was then spin-cast on the substrates. Based on their thermal properties, BOIBDD-2CN-C_{16} and BOIBDD-2CN-C_{17} based transistors were annealed in a nitrogen glovebox for 1 day at 130 and 75 °C, respectively. It is worth mentioning that the low annealing temperature for BOIBDD-2CN-C_{17} is compatible with flexible and inexpensive poly(ethylene terephthalate) (PET) substrates.

The output and transfer characteristics of the fabricated transistors were subsequently measured in air and under a stream of nitrogen by using a Keithley 4200 semiconductor analyzer. The field-effect mobility was extracted from the transfer curves obtained by using the standard transistor current−voltage equation in the saturation regime. Both BOIBDD-2CN-C_{16} and BOIBDD-2CN-C_{17} exhibited unipolar electron transport. Based on 10 devices, the average electron mobility of annealed BOIBDD-2CN-C_{16} and BOIBDD-2CN-C_{17} was about 0.015 and 0.1 $cm^2\ V^{-1}\ s^{-1}$, respectively. For comparison, unannealed transistors were also measured under the same conditions. As anticipated, the device performance was poor. The average electron mobility of BOIBDD-2CN-C_{16} and BOIBDD-2CN-C_{17} only reached 1.7×10^{-4} and 2.3×10^{-3}, respectively. The output and transfer characteristics of the annealed transistors are illustrated in Figure 6. As shown in Figure 6, the on/off ratios are above 10^5 for both materials and the threshold voltages are below 4 V, indicating low electron injection barriers even when high-work-function Au electrodes are used. The transistors are air stable, even without any encapsulation. The transistor comprising BOIBDD-2CN-C_{17} as the active layer was shown to exhibit an electron mobility of about 0.085 $cm^2/(V\ s)$ following 3 days of exposure to air. The observed stability was significantly better that that observed for commercially available high mobility *n*-type polymer P(NDI2OD-T2). Indeed, in bottom-contact and bottom-gated transistors, the performance of P(NDI2OD-T2) degraded within 1 h of air exposure. It is worth mentioning that BOIBDD-2CN-C_{17} outperforms BOIBDD-2CN-C_{16} in transistor applications. This can be well explained by the better intermolecular organization in the BOIBDD-2CN-C_{17} film, as shown by the UV−vis absorption, XRD, and AFM studies.

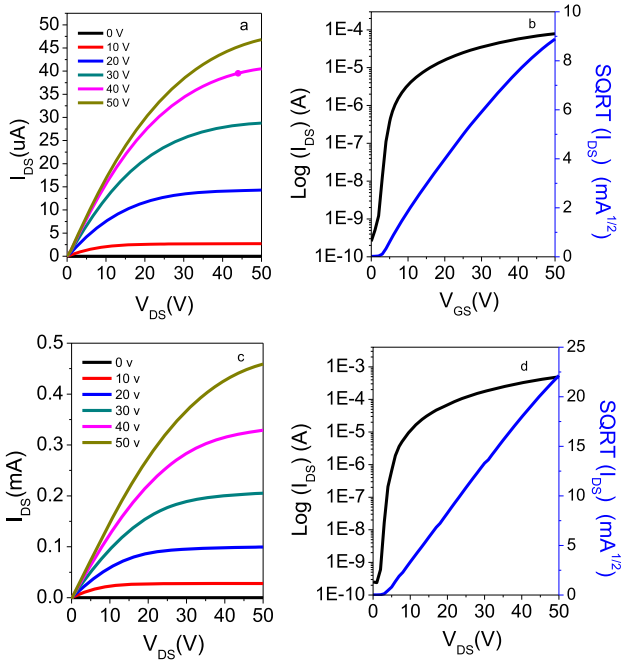

Figure 6. Output and transfer characteristics of the OFETs fabricated with BOIBDD-2CN-C_{16} (a, b) and BOIBDD-2CN-C_{17} (c, d) on OTS treated SiO_2/Si (W/L = 10000 μm/20 μm).

CONCLUSION

In summary, two unipolar n-type organic semiconductors based on dicyano-substituted bis(2-oxoindolin-3-ylidene)-benzodifurandione derivatives with engineered alkyl side chains, BOIBDD-2CN-C_{16} and BOIBDD-2CN-C_{17}, were synthesized and characterized. Cyano substitution was shown to be a more effective and cost-efficient way to lower the HOMO and LUMO energy levels of BOIBDD derivatives to achieve air-stable electron transport in solution-processed films. More interestingly, we found that a small change in the side chains (C_{16} vs C_{17}) resulted in remarkable changes in the physical properties and electronic performance of the organic semiconductors. BOIBDD-2CN-C_{17} exhibited a pronounced red-shift of 55 nm in the absorption peak from dichloromethane solution to the solid state, whereas BOIBDD-2CN-C_{16} showed a slight blue-shift of 13 nm. Both AFM and XRD studies confirmed that BOIBDD-2CN-C_{17} readily formed crystalline structures in the solid state prior to annealing. Furthermore, thermal annealing at a temperature as low as 75 °C, well below its melting point of 305 °C, can still improve the crystallinity of BOIBDD-2CN-C_{17} and thus significantly increase its electron mobility by 43 times to 0.1 $cm^2\ V^{-1}\ s^{-1}$ in air. This finding highlights the important role of side chains in tuning the performance and processability of small molecule based crystalline organic semiconductors.

ASSOCIATED CONTENT

Supporting Information

The Supporting Information is available free of charge at https://pubs.acs.org/doi/10.1021/acsaelm.9b00594.

NMR spectra, MALDI-TOF MS spectra, and elemental analysis results (PDF)

DOI: 10.1021/acsaelm.9b00594
ACS Appl. Electron. Mater. 2020, 2, 103−110

AUTHOR INFORMATION

Corresponding Authors

*E-mail: jianping.lu@nrc-cnrc.gc.ca.
*E-mail: ye.tao@nrc-cnrc.gc.ca.

ORCID

Jianping Lu: 0000-0003-3152-7510
Yuning Li: 0000-0003-3679-8133

Notes

The authors declare no competing financial interest.

ACKNOWLEDGMENTS

The authors thank Mr. Gilles Robertson, Mr. Kenneth Chan, Mr. Stephen Lang, Mr. Eric Estwick, and Mr. Hiroshi Fukutani for their technical support. The financial support from National Research Council Canada is greatly acknowledged.

REFERENCES

(1) Tang, C. W.; VanSlyke, S. A. Organic electroluminescent diodes. *Appl. Phys. Lett.* **1987**, *51*, 913−915.
(2) Cui, L.-S.; Deng, Y.-L.; Tsang, D.; Jiang, Z.-Q.; Zhang, Q.; Liao, L.-S.; Adachi, C. Controlling Synergistic Oxidation Processes for Efficient and Stable Blue Thermally Activated Delayed Fluorescence Devices. *Adv. Mater.* **2016**, *28*, 7620−7625.
(3) Yuan, Y.; Giri, G.; Ayzner, A. L.; Zoombelt, A. P.; Mannsfeld, S. C. B.; Chen, J.; Nordlund, D.; Toney, M. F.; Huang, J.; Bao, Z. Ultra-high mobility transparent organic thin film transistors grown by an off-centre spin-coating method. *Nat. Commun.* **2014**, *5*, 3005.
(4) Tseng, H.; Phan, H.; Luo, C.; Wang, M.; Perez, L. A.; Patel, S. N.; Ying, L.; Kramer, E. J.; Nguyen, T.; Bazan, G. C.; Heeger, A. J. High-mobility field-effect transistors fabricated with macroscopic aligned semiconducting polymers. *Adv. Mater.* **2014**, *26*, 2993−2998.
(5) Chu, T.-Y.; Lu, J.; Beaupre, S.; Zhang, J.; Pouliot, J.-R.; Wakim, S.; Zhou, J.; Leclerc, M.; Li, Z.; Ding, J.; Tao, Y. Bulk heterojunction solar cells using thieno[3,4-c]pyrrole-4,6-dione and dithieno[3,2-b:2′,3′-d]silole copolymer with a power conversion efficiency of 7.3%. *J. Am. Chem. Soc.* **2011**, *133*, 4250−4253.
(6) Cui, Y.; Yao, H.; Zhang, J.; Zhang, T.; Wang, Y.; Hong, L.; Xian, K.; Xu, B.; Zhang, S.; Peng, J.; Wei, Z.; Gao, F.; Hou, J. Over 16% efficiency organic photovoltaic cells enabled by a chlorinated acceptor with increased open-circuit voltages. *Nat. Commun.* **2019**, *10*, 2515.
(7) Yang, J. S.; Swager, T. M. Fluorescent Porous Polymer Films as TNT Chemosensors: Electronic and Structural Effects. *J. Am. Chem. Soc.* **1998**, *120*, 11864−11873.
(8) Bai, H.; Shi, G. Gas Sensors Based on Conducting Polymers. *Sensors* **2007**, *7*, 267−307.
(9) Yuan, J.; Zhang, Y.; Zhou, L.; Zhang, G.; Yip, H.-L.; Lau, T.-K.; Lu, X.; Zhu, C.; Peng, H.; Johnson, P. A.; Leclerc, M.; Cao, Y.; Ulanski, J.; Li, Y.; Zou, Y. Single-Junction Organic Solar Cell with over 15% Efficiency Using Fused-Ring Acceptor with Electron-Deficient Core. *Joule* **2019**, *3*, 1140−1151.
(10) Li, J.; Zhao, Y.; Tan, H.; Guo, Y.; Di, C.; Yu, G.; Liu, Y.; Lin, M.; Lim, S.; Zhou, Y.; Su, H.; Ong, B. A Stable Solution-Processed Polymer Semiconductor with Record High-Mobility for Printed Transistors. *Sci. Rep.* **2012**, *2*, 754.
(11) Zheng, Y.-Q.; Lei, T.; Dou, J.-H.; Xia, X.; Wang, J.-Y.; Liu, C.-J.; Pei, J. Strong Electron-Deficient Polymers Lead to High Electron Mobility in Air and Their Morphology-Dependent Transport Behaviors. *Adv. Mater.* **2016**, *28*, 7213−7219.
(12) Di Pietro, R.; Sirringhaus, H. High Resolution Optical Spectroscopy of Air-Induced Electrical Instabilities in n-type Polymer Semiconductors. *Adv. Mater.* **2012**, *24*, 3367−3372.
(13) Yan, H.; Chen, Z.; Zheng, Y.; Newman, C.; Quinn, J. R.; Dötz, F.; Kastler, M.; Facchetti, A. A High-Mobility Electron-Transporting Polymer for Printed Transistors. *Nature* **2009**, *457*, 679−686.
(14) Schuettfort, T.; Thomsen, L.; McNeill, C. R. Observation of a Distinct Surface Molecular Orientation in Films of a High Mobility Conjugated Polymer. *J. Am. Chem. Soc.* **2013**, *135*, 1092−1101.
(15) Dadvand, A.; Lu, J.; Py, C.; Chu, T.-Y.; Movileanu, R.; Tao, Y. Inkjet Printable and Low Annealing Temperature Gate-Dielectric Based on Polymethylsilsesquioxane for Flexible n-Channel OFETs. *Org. Electron.* **2016**, *30*, 213−218.
(16) Yan, Z.; Sun, B.; Li, Y. Novel Stable (3E,7E)-3,7-Bis(2-oxoindolin-3-ylidene)benzo[1,2-b:4,5-b′]difuran-2,6(3H,7H)-dione Based Donor−Acceptor Polymer Semiconductors for n-Type Organic Thin Film Transistors. *Chem. Commun.* **2013**, *49*, 3790−3792.
(17) He, Y.; Guo, C.; Sun, B.; Quinn, J.; Li, Y. Branched Alkyl Ester Side Chains Rendering Large Polycyclic (3E,7E)-3,7-Bis(2-oxoindolin-3-ylidene)benzo[1,2-b:4,5-b′]difuran-2,6(3H,7H)-dione (IBDF) Based Donor−Acceptor Polymers Solution-Processability for Organic Thin Film Transistors. *Polym. Chem.* **2015**, *6*, 6689−6697.
(18) Lei, T.; Xia, X.; Wang, J.; Liu, C.; Pei, J. Conformation Locked" Strong Electron-Deficient Poly(p-Phenylene Vinylene) Derivatives for Ambient-Stable n-Type Field-Effect Transistors: Synthesis, Properties, and Effects of Fluorine Substitution Position. *J. Am. Chem. Soc.* **2014**, *136*, 2135−2141.
(19) Dou, J.; Zheng, Y.; Yao, Z.; Yu, Z.; Lei, T.; Shen, X.; Luo, X.; Sun, J.; Zhang, S.; Ding, Y.; Han, G.; Yi, Y.; Wang, J.; Pei, J. Fine-Tuning of Crystal Packing and Charge Transport Properties of BDOPV Derivatives through Fluorine Substitution. *J. Am. Chem. Soc.* **2015**, *137*, 15947−15956.
(20) Liu, M. S.; Jiang, X.; Liu, S.; Herguth, P.; Jen, A. K.-Y. Effect of cyano substituents on electron affinity and electron-transporting properties of conjugated polymers. *Macromolecules* **2002**, *35*, 3532−3538.
(21) Wang, H.; Huang, J.; Uddin, M. A.; Liu, B.; Chen, P.; Shi, S.; Tang, Y.; Xing, G.; Zhang, S.; Woo, H. Y.; Guo, H.; Guo, X. Cyano-Substituted Head-to-Head Polythiophenes: Enabling High-Performance *n*-Type Organic Thin-Film Transistors. *ACS Appl. Mater. Interfaces* **2019**, *11*, 10089−10098.
(22) Alem, S.; Wakim, S.; Lu, J.; Robertson, G.; Ding, J.; Tao, Y. Degradation Mechanism of Benzodithiophene-Based Conjugated Polymers when Exposed to Light in Air. *ACS Appl. Mater. Interfaces* **2012**, *4*, 2993−2998.
(23) Meager, I.; Ashraf, R. S.; Mollinger, S.; Schroeder, B. C.; Bronstein, H.; Beatrup, D.; Vezie, M. S.; Kirchartz, T.; Salleo, A.; Nelson, J.; McCulloch, I. Photocurrent Enhancement from Diketopyrrolopyrrole Polymer Solar Cells through Alkyl-Chain Branching Point Manipulation. *J. Am. Chem. Soc.* **2013**, *135*, 11537−11540.
(24) Lu, J.; Dadvand, A.; Chu, T.; Movileanu, R.; Baribeau, J.; Ding, J.; Tao, Y. Inkjet-printed unipolar n-type transistors on polymer substrates based on dicyanomethylene-substituted diketopyrrolopyrrole quinoidal compounds. *Org. Electron.* **2018**, *63*, 267−275.
(25) Lei, T.; Dou, J.; Pei, J. Influence of Alkyl Chain Branching Positions on the Hole Mobilities of Polymer Thin-Film Transistors. *Adv. Mater.* **2012**, *24*, 6457−6461.
(26) Mei, J.; Kim, D. H.; Ayzner, A. L.; Toney, M. F.; Bao, Z. Siloxane-Terminated Solubilizing Side Chains: Bringing Conjugated Polymer Backbones Closer and Boosting Hole Mobilities in Thin-Film Transistors. *J. Am. Chem. Soc.* **2011**, *133*, 20130−20133.
(27) Guo, Y.; Jin, Y.; Su, Z. Spectroscopic study of side-chain melting and crystallization of regioregular poly(3-dodecylthiophene). *Polym. Chem.* **2012**, *3*, 861−864.

DOI: 10.1021/acsaelm.9b00594
ACS Appl. Electron. Mater. 2020, 2, 103−110